

We are IntechOpen, the world's leading publisher of Open Access books Built by scientists, for scientists

6,900

Open access books available

186,000

International authors and editors

200M

Downloads

Our authors are among the

154

Countries delivered to

TOP 1%

most cited scientists

12.2%

Contributors from top 500 universities



WEB OF SCIENCE™

Selection of our books indexed in the Book Citation Index
in Web of Science™ Core Collection (BKCI)

Interested in publishing with us?
Contact book.department@intechopen.com

Numbers displayed above are based on latest data collected.
For more information visit www.intechopen.com



New Trends in Active Power Filter for Modern Power Grids

Luís Fernando Corrêa Monteiro

Additional information is available at the end of the chapter

<http://dx.doi.org/10.5772/intechopen.72195>

Abstract

From harmonic compensation to interface with renewable energy sources, active filters are capable to improve power quality, increase the reliability of the power grid, and contribute to make feasible the implementation of decentralized microgrids. In this scenario, this chapter provides a discussion involving new trends on distribution power grids, with active power filters playing an important key role. Considering the aforementioned explanation, part of the chapter covers active filter applications for power grids. In sequence, we discuss time domain control algorithms to identify power quality disturbances or other problems that may compromise the power grid reliability, with simulation results to evaluate the performance of the active filters for compensating power quality problems under transient- and steady-state conditions. Next, we discuss the integration of active filters with renewable energy sources (REs) including a brief explanation of maximum power point tracking (MPPT) algorithms and other controllers considering a decentralized microgrid scenario with several active filters connected at the same grid circuit.

Keywords: active filters, current and voltage compensation, real-time algorithms, renewable energy sources, microgrids

1. Introduction

In this section, we present a discussion involving basic aspects of the active filters for generation and distribution grids. It is important to comment that there are also power electronics compensators for transmission grids presenting different features as, for instance, damping subsynchronous resonance [1], power flow control [2, 3] and improve the stability of a power system [4]. These compensators are known as Flexible AC Transmission System (FACTS), and their study is beyond the scope of this chapter.

Backing to the active power filters, they can be understood as a controlled current sources or controlled voltage sources capable for compensating different power quality problems as, for

instance, harmonic and unbalanced components, power factor, voltage sags or swells, damping low-frequency harmonic oscillations, and so on [5, 6]. Moreover, they are used as an interface for renewable energy sources in a new concept of distributed generation or even making the implementation of decentralized microgrids reliable [7–9].

A simplified scheme of the shunt active filter compensating all the harmonic currents drawn by the load is illustrated in **Figure 1**. An active filter is comprehended by power and control stages. The power stage comprises a voltage source converter (VSI), with a storage energy element (capacitor) at its DC link, inductor filter (L_{fp}), and small passive filters (Z_{fp}) to provide a low impedance path to the high-frequency components of the produced current by the VSI (i_{Lfp}). The control stage presents measurement and instrumentation circuits, microcontrollers, and VSI drivers. As indicated in **Figure 1**, the reference current produced by the VSI (i^*) is determined based on the applied control algorithms, which presents the load current (i_L), grid voltage (v_S) and the DC-link voltage (v_{DC}) as inputs. There is also a pwm controller for keeping i_{Lfp} in conformity with the reference current (i^*). A common point (**cp**) was considered to indicate that, in a three-phase circuit, the passive filters are connected at this point of the circuit.

It is important to comment that an inductor (L_S) is usually applied to represent the grid impedance, which reflects the inductance characteristics of line cables and power transformers. Nevertheless, current researches point out to replace its representation by equivalent impedances that are dynamically modified due to a considerable amount of nonlinear loads, which are dynamically connected and removed from the power grid. This issue becomes more important nowadays due to the proliferation of renewable energy sources with power converter interface [10–13].

Figure 2 illustrates a simplified scheme of the series active filter compensating harmonics and voltage sag, with the reference voltage (v^*) being determined through the applied control algorithms, which presents the grid current (i_S), grid voltage (v_S), and the DC-link voltage (v_{DC}) as inputs. Moreover, there is a pwm controller for producing the VSI filtered voltage (v_{Zsf}).

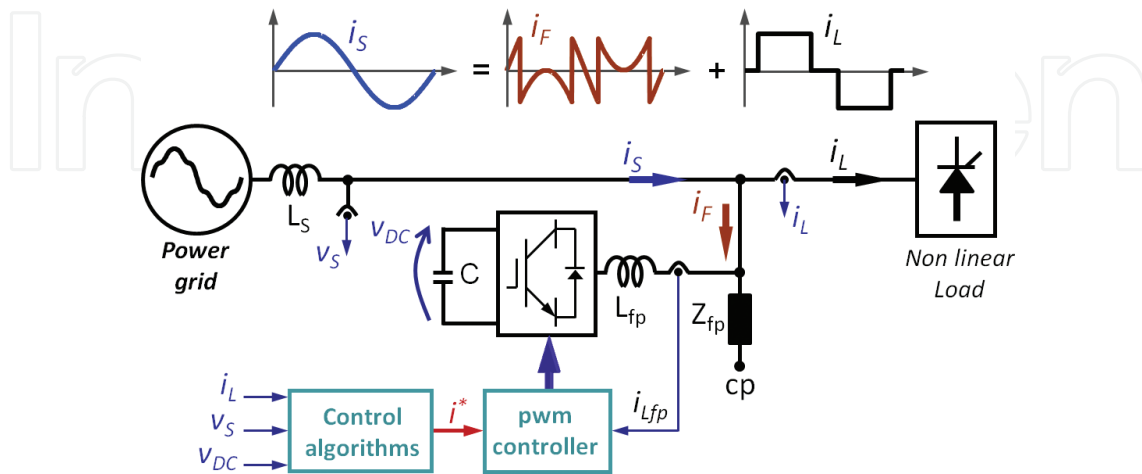


Figure 1. Simplified scheme of the shunt active filter compensating all the harmonic currents drawn by the nonlinear load.

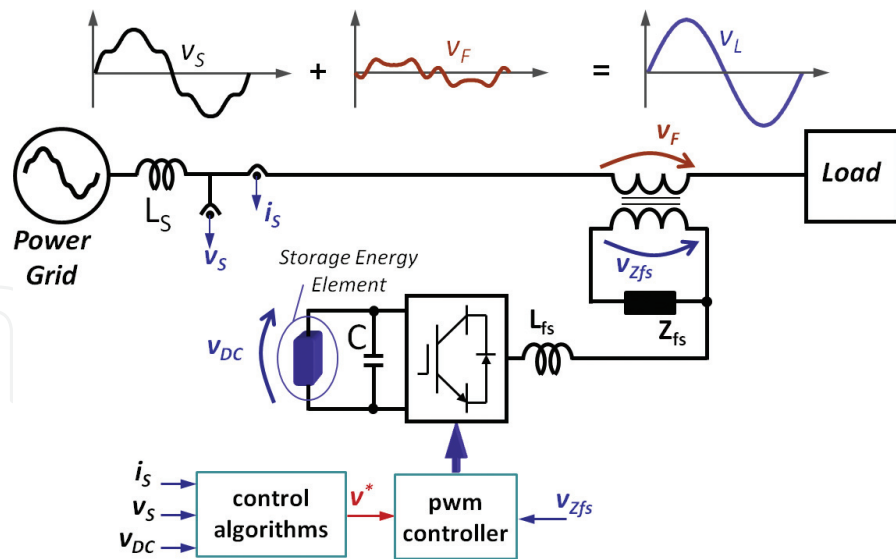


Figure 2. Simplified scheme of the series active filter compensating harmonics and voltage sag.

An additional storage energy element (SEE) is necessary if sag compensation is required. As depicted **Figure 2** with a SEE connected in parallel with the DC-link capacitor, it can be represented as, for instance, ultracapacitors or batteries [14]. There are also other SEEs as superconducting magnetic energy storage (SMES) [15] and flywheel [16]. However, once they are not voltage-source type, it is necessary to use power converters to interface them with the DC-link voltage.

Other issue involving the power stage of the series active filter corresponds to its series connection, which may or may not be done through power transformers. A constraint for implementing active filters without series transformer injection is to avoid short circuits between the phase circuits, which can be done replacing the three-phase VSI by three single-phases VSIs with three independent DC-link voltages as introduced in [17, 18]. Other alternative is the use of high-frequency transformers at the DC-link of the single-phase VSIs, which are usually applied in isolated DC-DC converters [19].

Other possible active filter topology consists on the combination of the shunt and series active filters, resulting on the unified power quality conditioner (UPQC). As described in [20], by having these two conditioners connected to the electrical system, simultaneous compensation of the current demanded from the utility and the voltage delivered to the load can be accomplished. As illustrated in **Figure 3**, the series and shunt active filters compensate at the same time all the harmonic components of the load currents and grid voltages. Its power stage combines all the passive components of the series and shunt active filters as previously exploited. In the same way, its control stage presents all the circuitry, microcontrollers, and control algorithms of both active filters. Particularly, in this configuration, the shunt active filter is responsible to draw a controlled current to keep the DC-link voltage (v_{DC}) regulated. A summary of the UPQC compensation capabilities is shown in **Table 1**, with the functionalities of the series and shunt active filters well established. Nevertheless, there are proposals in the literature with both active filters compensating the same power quality problem in a complementary way. For instance [21, 22]

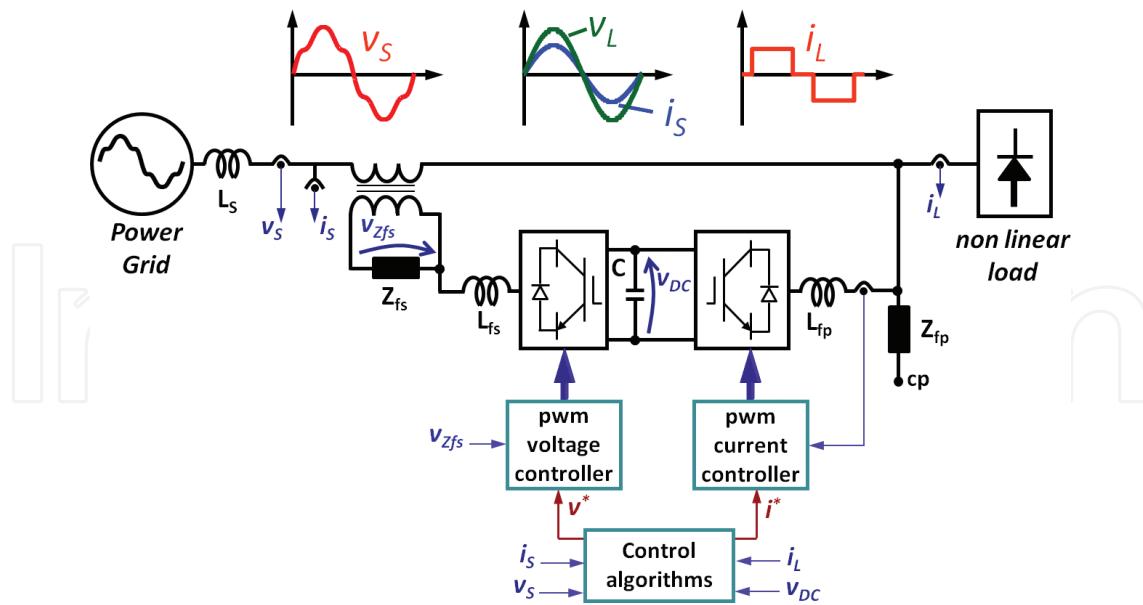


Figure 3. Simplified scheme of the unified power quality conditioner (UPQC).

Active filter	Functionality
Series active filter	Harmonic and unbalanced voltages compensation Voltage sags/swells compensation Improvement of the power grid stability
Shunt active filter	Harmonic and unbalanced currents compensation Power factor correction

Table 1. UPQC functionalities.

present a sag compensation proposal through the combined operation of the series and shunt active filters for the maximum utilization of both active filters.

In next section, we exploit their control algorithms.

2. Overview of active power filters for current and voltage compensation

Due to the power grid dynamics, an instantaneous or, at least, a quasi-instantaneous response of the active filters is desirable, which leads the use of time domain control algorithms together with synchronizing circuits. Hence, in this section, we exploit control algorithms to the series- and shunt-active filters with simulation results.

2.1. Control algorithms for shunt active filter

Basically, control algorithms for shunt active filters can be divided into a set of algorithms for determining the reference current and other algorithms for controlling the produced current by the VSI, which depends on the applied switching technique.

Algorithms for determining the reference current are related to which features we expect that the active filter be able to compensate. It is important to comment that control algorithms for shunt active filters have been proposed in the literature for more than 30 years. Among all these proposals, those derived from the instantaneous power theory [23–25], dq reference frame [26–28], conservative power theory [7], and the active and non-active currents [29–31] are widely applied.

The instantaneous power theory, or p-q theory, was emerged at the beginning of the 1980s, with the main purpose to provide new power definitions in time domain for three-phase three-wire circuits and, in sequence for three-phase four-wire circuits. Based on the $\alpha\beta 0$ system coordinates, the p-q theory has the advantage of instantaneously separating the homopolar (zero-sequence) from the nonhomopolar (positive- and negative-sequence) components [31]. This issue allowed new proposals on control algorithms to three-phase four-wire active filters. An enhanced version of the p-q theory, known as the $p-q-r$ theory, was conceived based on a different coordinate translation, where voltages and currents are translated from $\alpha\beta 0$ to $p-q-r$ system coordinates [32, 33]. Another approach is the use of Park transformation with a synchronizing circuit (d-q coordinate system) to conceive control algorithms based on the dq reference frame. A comparison involving all of these algorithms for active power filters was introduced in [33].

A different methodology from the aforementioned corresponds to the active and non-active currents, which does not present any kind of coordinate translation. It derives from Fryze active current concept and presents a very simple formulation as introduced in [34]. Essentially, this algorithm determines the minimum (active) current component that transports the same energy of a generic three-phase load current. Due to its simplicity, we choose the control algorithms based on the active and non-active currents as basis to exploit the performance of the active filters, considering a power grid with unbalanced voltages and nonlinear loads.

Figure 4 presents a control algorithm for constant instantaneous active power concept, whereas **Figure 5** for sinusoidal grid current concept, with the grid voltages (v_{sa} , v_{sb} , v_{sc}) replaced by the control signals pll_a , pll_b , pll_c . These signals are unitary sinusoidal waveforms synchronized with the fundamental positive-sequence component of the grid voltages

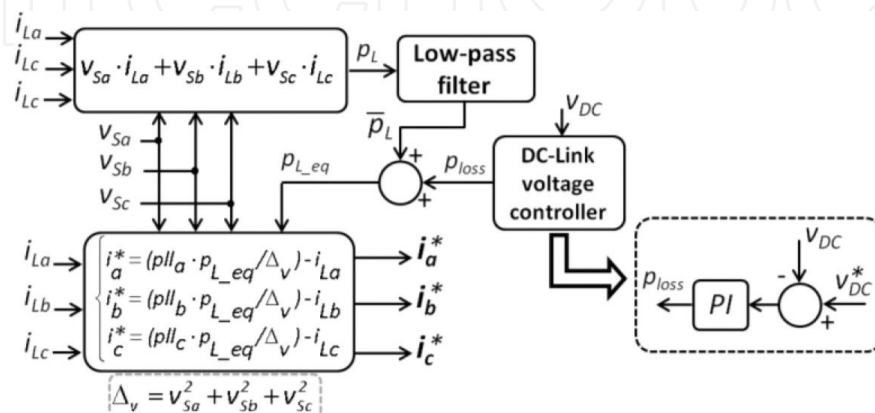


Figure 4. Control algorithm based on the Fryze active currents for constant instantaneous active power concept.

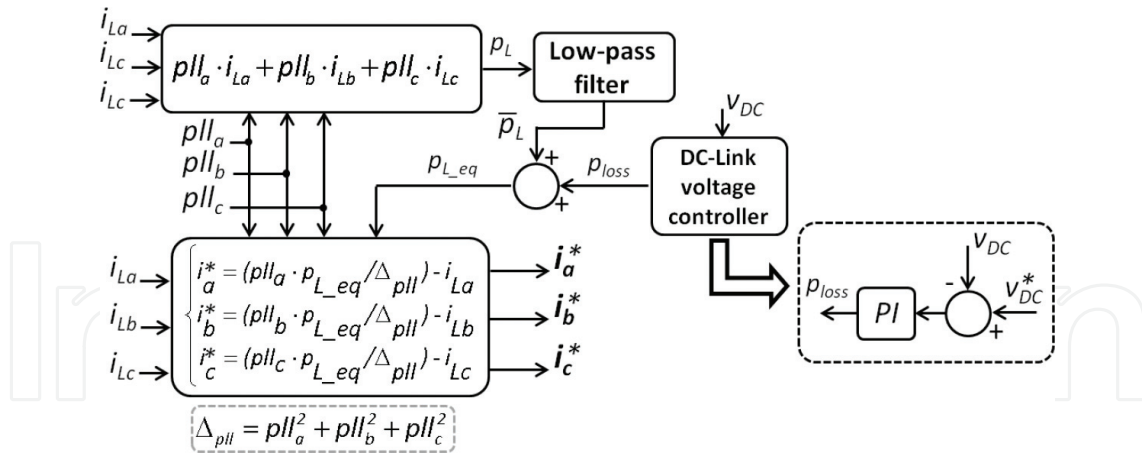


Figure 5. Control algorithm based on the Fryze active currents for sinusoidal grid current concept.

(v_{Sa} , v_{Sb} , v_{Sc}), and they were obtained through a PLL circuit [35–38]. It is important to highlight that when sinusoidal grid currents are required, considering unbalanced or distorted grid voltages, a circuit capable to extract the fundamental positive-sequence component of the grid voltages must be added to the control algorithm of the active filter, independently of the chosen methodology.

Based on both control algorithms, one can see that the control signal p_L presents different meanings. Indeed, for constant instantaneous power concept (Figure 4), p_L derives from the active power of the grid, whereas for sinusoidal current concept (Figure 5), p_L derives from the active power involving the fundamental positive-sequence component of the load currents only.

This issue can be better understood through the illustrated results in Figures 6 and 7. According to the simulation results in Figure 6, for providing constant active power, the compensated grid current still presents some harmonic components from the load current. It is important to comment that, according to the definitions proposed by Fryze, p_{grid} corresponds to the active power, whereas all the other components represent the non-active power. In this case study, there is only active power due to applied control algorithm.

On the other hand, as shown in Figure 7, the compensated current is sinusoidal even with a distorted grid voltage. Moreover, once the average component of q_{grid} is equal to zero, it is possible to affirm that the compensated current is in phase with the fundamental positive-sequence component of the grid voltage. A negative aspect of this concept is the presence of oscillating components at p_{grid} and q_{grid} , which may compromise the performance of other equipment and devices connected to this power grid, where the active power corresponds to the average component of p_{grid} , with the remaining components representing the non-active power.

Particularly, for minimizing the involved costs of the active filter, one can consider selective harmonic filtering as a feasible possibility. In this case, the compensation of a few harmonic components, especially the lower harmonic orders (third and fifth harmonics, for instance), may result in the compensated grid current with a total harmonic distortion (THD) lower than

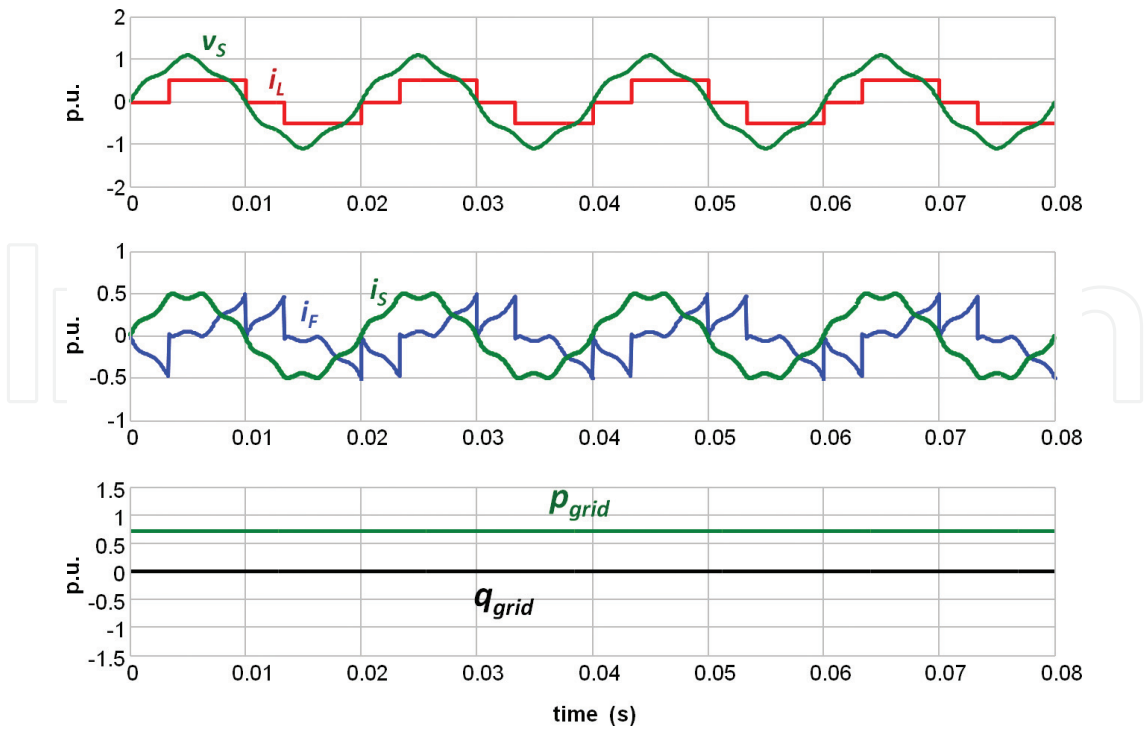


Figure 6. Simulation results with the control algorithm based on the constant active power concept.

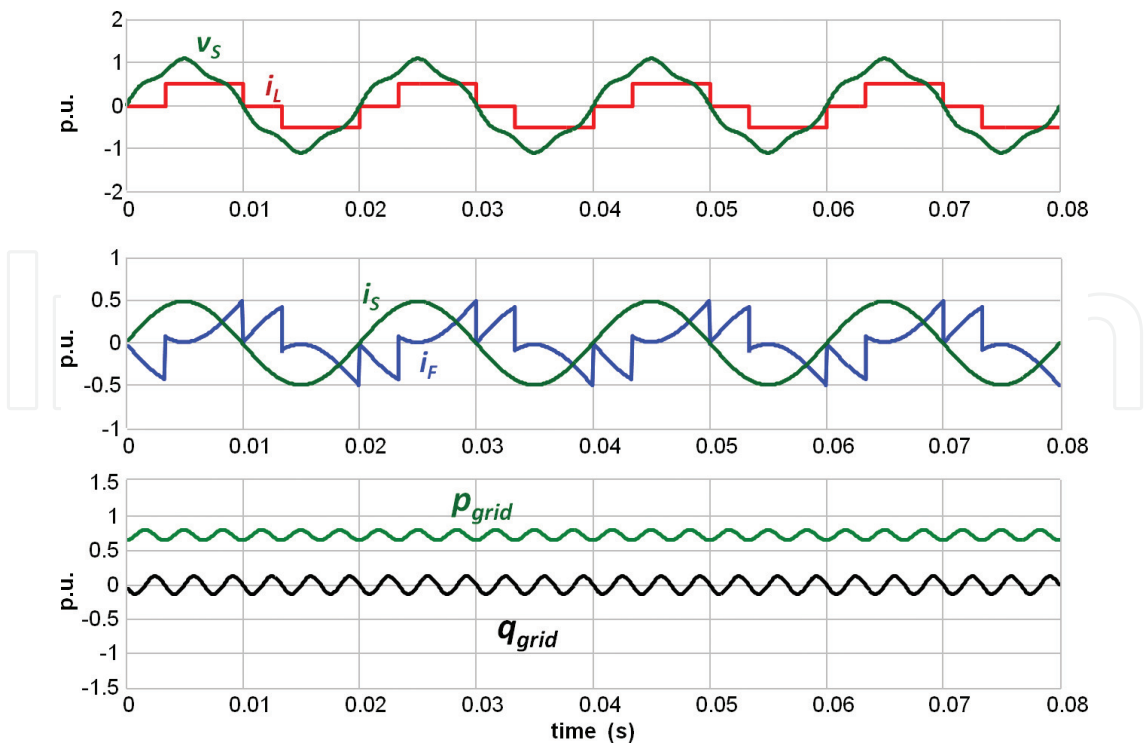


Figure 7. Simulation results with the control algorithm based on the sinusoidal grid current concept.

5%, which is acceptable for most of power quality norms and recommendations. Other possibility is to replace the compensation of a specific harmonic component by a harmonic symmetrical component, in case of unbalance load currents, as proposed in [39].

2.2. Control algorithms for series active filter

As depicted in **Figure 8**, the main control algorithms to the series active filter comprehend a PLL circuit, an algorithm to extract the fundamental positive-sequence component of the grid voltages, the DC-link voltage controller, and a damping algorithm. With these control algorithms, the series active filter is able to provide full compensation of harmonics and unbalanced components; and moreover, it is also capable to improve the power grid stability through the damping controller. In sequence, the algorithm for determining the positive-sequence component of the grid voltages and the damping algorithm are exploited.

According to the block diagrams illustrated in **Figure 9**, one can see a similar methodology for determining the control signals, v_{S1+_a} , v_{S1+_b} , v_{S1+_c} , when compared with the one applied for determining the reference currents of the shunt active filter, based on the sinusoidal grid current concept.

A preliminary result of the series active filter is illustrated in **Figure 10**. With the introduced control algorithms shown in **Figure 8**, the amplitude of the compensated grid voltage is slightly decreased. It occurs due to the amount of energy necessary for keeping the DC-link voltage regulated, which is directly related to the power losses of the VSI and the small passive filters as well.

As alternative to mitigate this problem, one can consider the addition of an algorithm to obtain a controlled voltage in quadrature with the control signals v_{S1+_a} , v_{S1+_b} , v_{S1+_c} . It is important to comment that these added voltages do not produce active power with the grid currents, and, consequently, they do not interfere on the flow of energy between the active filter with the power grid. A block diagram of this algorithm is shown in **Figure 11**, where the amplitude

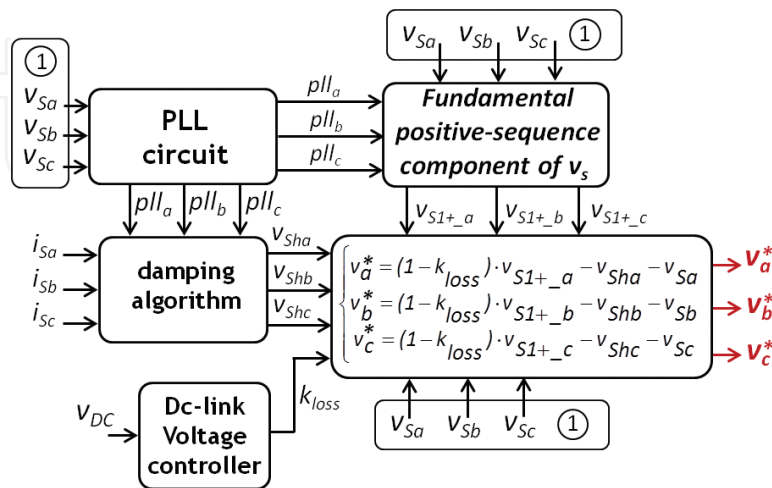


Figure 8. Block diagrams of the control algorithms to the series active filter, with damping controller and DC-link voltage controller.

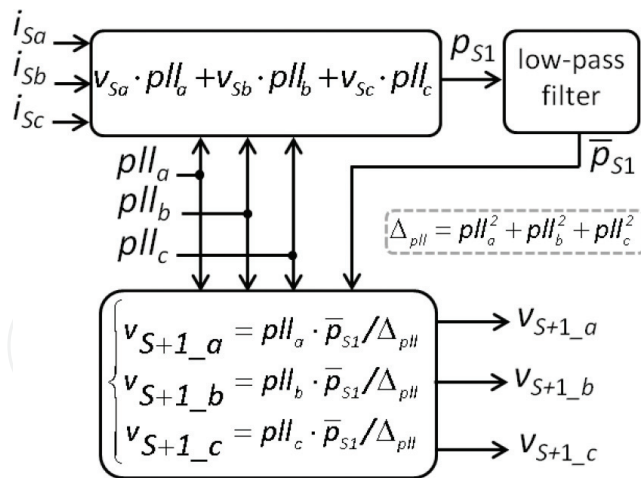


Figure 9. Block diagrams of the algorithm to determine the fundamental positive-sequence component of the grid voltage.

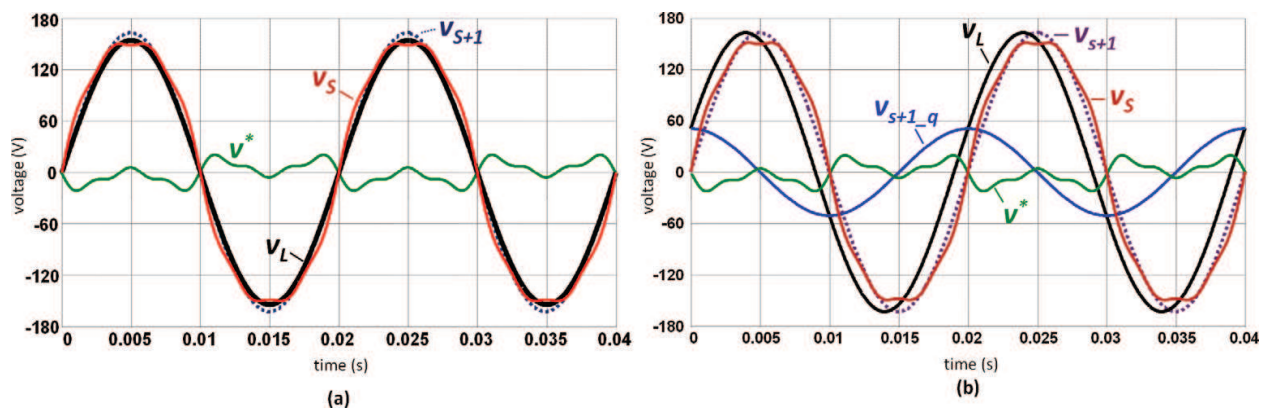


Figure 10. Preliminary results of the series active filter (a) with the control algorithms introduced in Figure 8 and (b) adding an algorithm for compensating the drop voltage derived from the DC-link voltage controller.

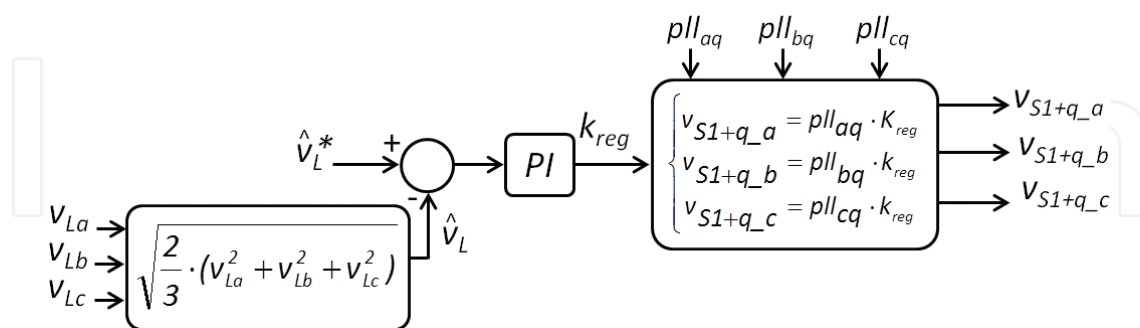


Figure 11. Block diagrams of the algorithm for determining controlled voltages in quadrature with the fundamental positive-sequence component of the grid voltages.

reference of the load voltages is compared with their aggregated value, being the amplitude of the controlled voltages determined by this algorithm. Furthermore, the control signals pll_{aq} , pll_{bq} , pll_{cq} are determined through the PLL circuit, which are unitary sinusoidal waveforms leading the control signals pll_a , pll_b , pll_c by 90° .

In case of adding tuned passive filters together with the series active filter, some constraints must be taken into account. In this topology, the passive filters provide a low impedance path to some of the harmonic components of the load currents, improving the performance of the series active filter. On the other hand, instability problems due to resonance phenomena involving the passive filters with the grid impedance may occur. An alternative to overcome this problem is to add the damping algorithm [29]. Through this algorithm, the series active filter produces a controlled voltage that behaves as a resistance to the harmonic currents that should be drawn by the passive filters.

Based on the block diagrams illustrated in **Figure 12**, the damping voltages (v_{Sha} , v_{Shb} , v_{Shc}) results from the direct product involving the non-active components of the grid currents (i_{Sha} , i_{Shb} , i_{Shc}) with the controlled signal R_h that can be understood as a controlled resistance to the non-active currents. Nevertheless, note that R_h must be designed for providing a controlled resistance to the non-active currents only. Otherwise it may compromise the flow of the active component of the grid current.

In sequence, we provide simulation results from a test case of the series active filter combined with shunt passive filters, as shown in **Figure 13**. The nonlinear load corresponds to the six-pulse thyristor bridge rectifier and the passive filters comprehend two selective passive filters at fifth and seventh harmonics, plus a passive filter for high-order harmonics. In this test case, while the active filter was turned OFF, there was a resonance among the passive filters with the grid impedance with some undesirable effects as, for example, distorted grid voltages (**Figure 13a**). When the active was turned ON, the resonance was damped in a time period lower than one cycle period (**Figure 13b**), with the active filter providing a controlled resistance to the non-active components of the grid current and, as a consequence, the active and passive filters presented a better performance as illustrated in **Figure 13c** and **d**, respectively. In this test case, at steady state, the THD of the grid currents decreased from 35% to less than 5%, which is acceptable by most of recommendations and norms related to power quality indexes.

2.3. Control algorithms for unified power quality conditioner

Essentially, the UPQC control algorithms combine those from the series and the shunt active filters with simplifications. Indeed, as illustrated in **Figure 14**, the UPQC control algorithms

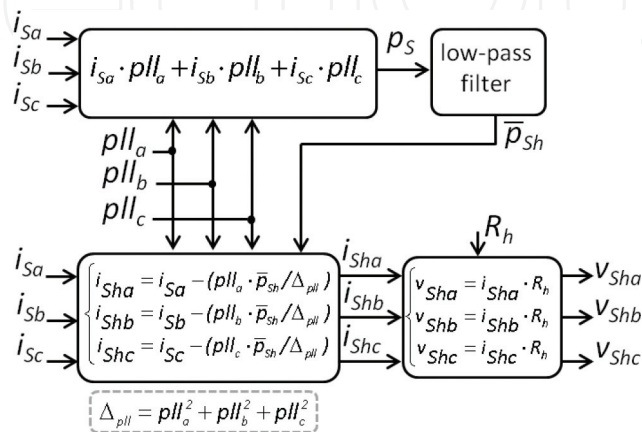


Figure 12. Block diagrams of the damping algorithm.

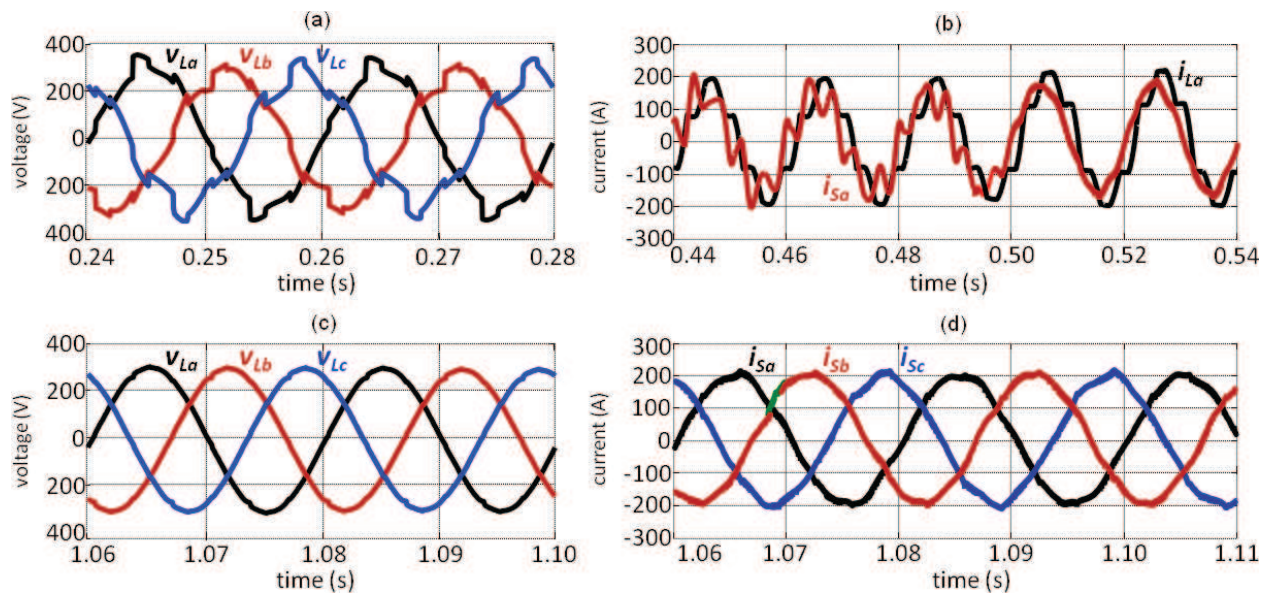


Figure 13. Simulation results of the series active filter combined with shunt passive filters; (a) load voltages with the active filter turned OFF, (b) grid and load currents at the transient when the active filter is turned ON, (c) load voltages with the active filter turned on under steady state, and (d) grid currents with the active filter turned on under steady state.

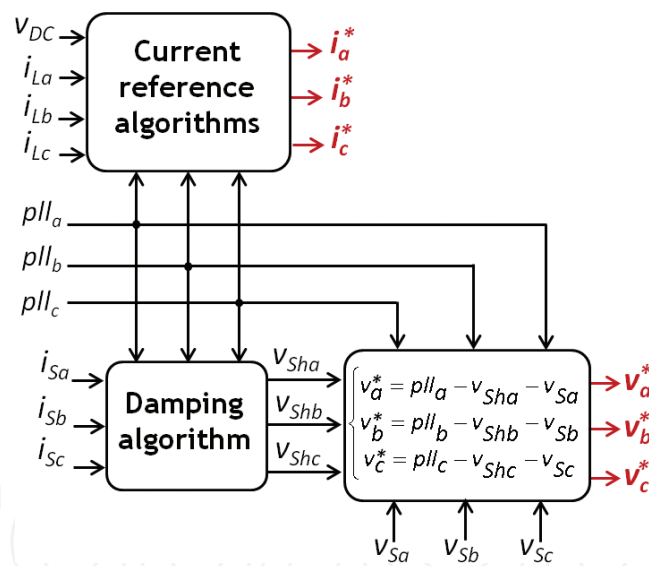


Figure 14. Block diagrams of the unified power quality conditioner.

comprehend the control algorithms of the shunt active filter, with a PLL circuit and the damping algorithm. The reference voltages are determined from a combination involving the grid voltages and the output signals of the damping algorithm and the PLL circuit.

Note that the algorithm to determine the fundamental positive sequence of the grid voltages was removed, with their outputs replaced by the PLL output signals. Indeed, if the measured system voltage is normalized such that an unity amplitude represents its nominal value, this normalized voltage signal can be directly compared with the PLL output to achieve the compensating voltage references. In this case, the difference between the PLL outputs and the

normalized voltages includes also sags or swells, as well as imbalances and distortions, which may be affecting the grid voltages.

Basically, to cover the power losses of the UPQC converters and the compensation of voltage sag or voltage swell, the shunt active filter produces a controlled current to keep the DC-link voltage regulated, with the amplitude of the grid currents being dynamically modified according to the UPQC power losses and the short duration voltage variations (SDVVs) compensated the series active filter as well.

Simulation results exploiting the UPQC compensation capabilities are shown in **Figures 15** and **16**. The nonlinear load corresponds to the 12-pulse thyristor bridge rectifier, and an unbalanced load was connected and removed from the power grid. One can see the capability of the shunt active filter compensating the harmonic and unbalance components of the load currents, with the compensated grid currents with low harmonic distortion (THD lower than 3%) and balanced. There is a dynamics at the amplitude of the grid currents due to the low-pass filter and the DC-link voltage controller as well. Based on the acquired results, it has taken more than 100 ms to the grid currents to reach their novel steady-state condition when a transient at the load current has occurred.

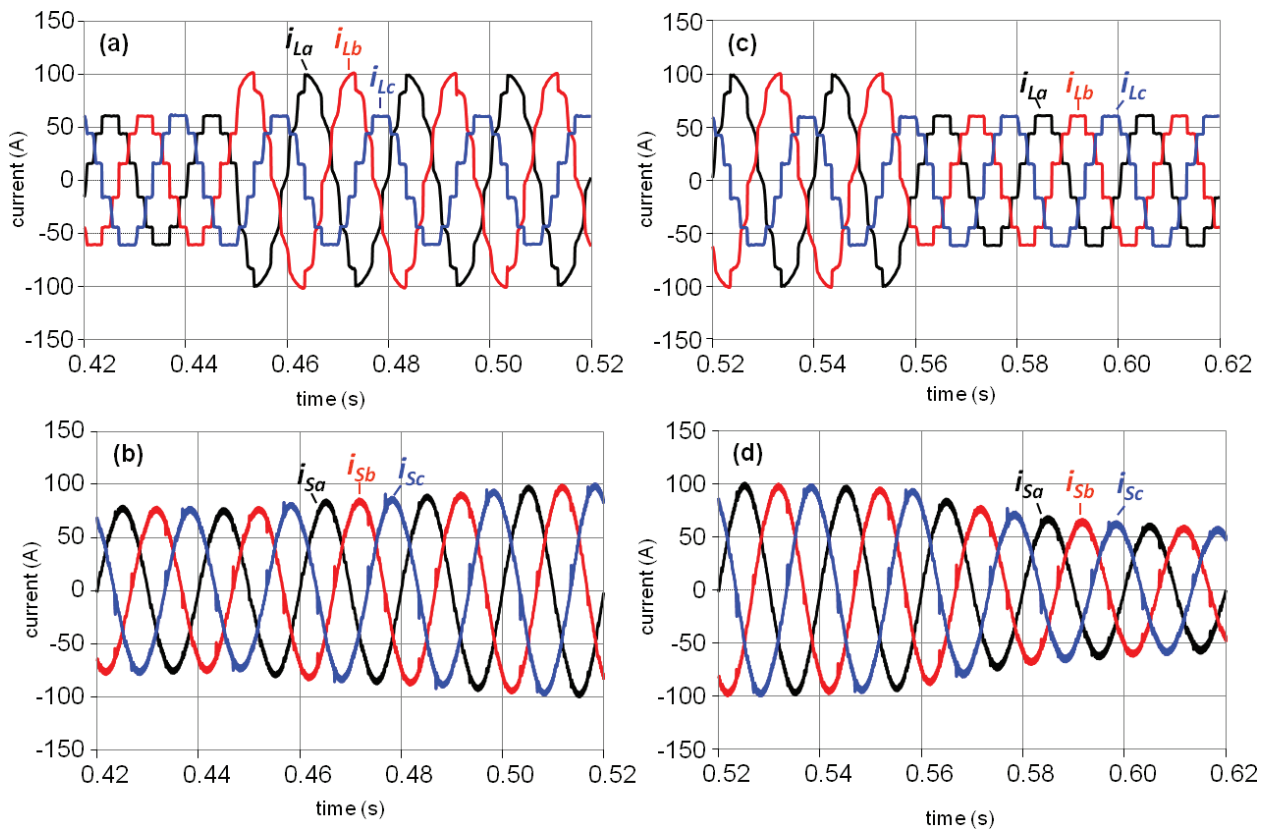


Figure 15. Simulation results of the UPQC shunt converter: (a) distorted load currents at the time transient when the unbalanced load was connected; (b) compensated grid currents at the transient when the unbalance load was connected; (c) distorted load currents at the transient when the unbalanced load was removed; and (d) compensated grid-currents at the transient when the unbalanced load was removed.

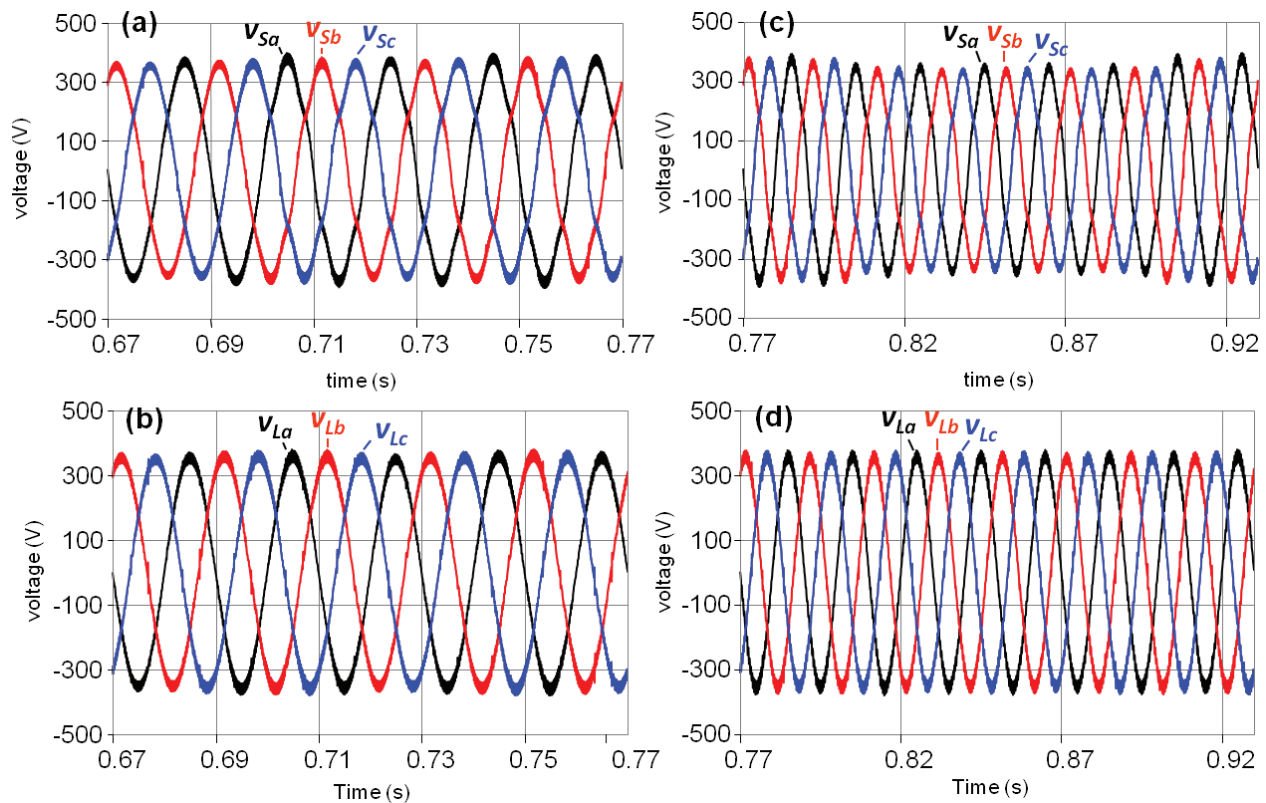


Figure 16. Simulation results of the UPQC series converter: (a) distorted grid voltages at the time transient when they become unbalanced; (b) compensated load voltages at the transient when the distorted grid voltages become unbalanced; (c) distorted and unbalanced grid voltages at the transient when a voltage sag occurs; (d) compensated load voltages at the transient when a voltage sag occurs.

Figure 16 illustrates the performance of series active filter compensating harmonic and unbalanced components at the grid voltage and a voltage sag occurrence. It can be noted a faster dynamic response of the series active filter, in comparison with the shunt active filter, once the series active filter is not affected by the DC-link voltage dynamics, enabling a quasi-instantaneous capability for transient compensation as shown in **Figure 16b** and **d**. In this section, we could verify the capability of the active filters for compensating most of the power quality problems. Nevertheless, there is another feature of them considered to be as interface for renewable energy sources, particularly, to the photovoltaic panels and wind systems as extremely diffused in the literature. This issue is exploited in the next section.

3. Integrating active power filters with renewable energy sources

Researches on high-performance power electronic converters combined with renewable energy sources (RENs) capable to extract more energy at a lower cost leads this technology to become technically and economically feasible to meet all the global energy needs. Encompassed by this course of events, there is a novel tendency for replacing the conventional centralized generation systems, with long transmission lines, to the distributed generation (DG) systems. In this novel concept on DG systems, renewable energy sources and storage

systems are combined with the existent conventional sources to supply stand-alone or grid-connected loads. Moreover, it provides a better way of using onsite energy resources, minimizing transmission and distribution costs, which is crucial to reduce obstacles for rural or remote areas electrification and to encourage sustainable business development.

In this scenario, which comprehends the real modern power grids, active filters play a key role as an interface for connecting the REN to the power grid. For example, consider the shunt active filter illustrated in **Figure 1** with photovoltaic panels and a DC-DC converter connected at the DC-link voltage, as indicated in **Figure 17**, and the shunt active filter presents an additional feature of controlling the produced energy of the photovoltaic panels to the power grid. Usually, there is a boost converter between the photovoltaic panels and the DC-link voltage (v_{DC}), once the terminal voltage on these panels is much lower than v_{DC} .

For extracting the maximum energy of these panels, the maximum power point tracking (MPPT) algorithm controls the duty cycle of the boost converter. Through the combined operation between the MPPT algorithm and the DC-link voltage controller, it is possible to control the exchange of energy from the PV to the power grid [40]. Consider the output signal of the DC-link voltage controller, labeled in **Figure 4** as P_{loss} , to understand this dynamics. In this scenario, once the produced current by the PV arrays exceeds the active power losses of the converters, P_{loss} becomes naturally negative. In this power balance, the duty cycle control of the MPPT algorithm increases while the derivative of the PV active power is positive, with the control signal P_{loss} becomes more negative to keep the DC-link voltage regulated at its rated value. This interactive loop stops when the derivative of the PV active power is equal to zero, which means that the optimal set point (MPPT) was reached. To avoid loss of controllability, it is recommended to include an enable condition to update the duty cycle output of the MPPT

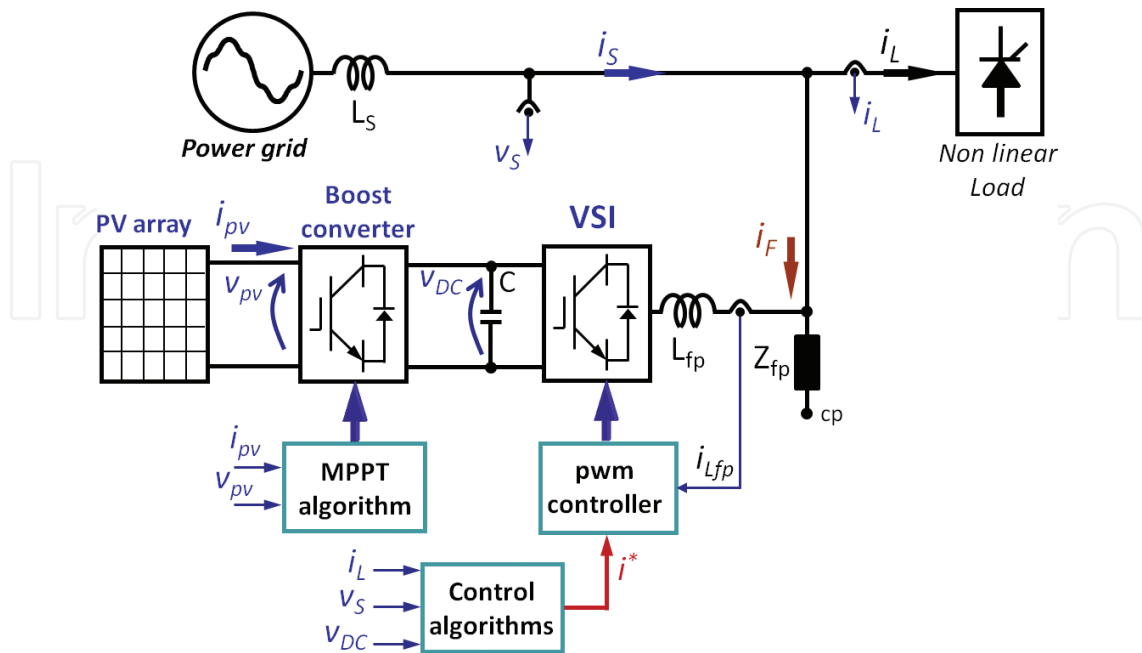


Figure 17. Shunt active filter as an interface for connecting photovoltaic panels to the power grid.

certain limits, through the shunt active filters with an energy storage element, capable to confine the oscillating energy between the active filter and the load [31].

Other issue is the load power sharing between different power converters in a decentralized microgrid. An alternative to overcome this problem is extending the droop controller concept to the shunt active filters connected in the same power grid. In this case, the active filters modify their output impedance through the virtual impedance method [42]. Basically, once these active filters share the same grid voltage, they are conditioned to produce controlled currents such that their output impedance is modified according to the capabilities of sharing the active- and reactive powers of the load. This issue is one of the most exploited ones by researchers to make the implementation of decentralized microgrids reliable.

4. Conclusions

Through this chapter, one can see the active filters capability for improving the power quality indexes due to their capability of producing, in almost real-time, controlled currents and voltages as verified through simulation results of the shunt active filter, series active filter, and the unified power quality conditioner compensating different power quality problems. Moreover, they play a key role integrating RENS to the power grid in a new concept of distributed generation (DG) systems, conditioning them to produce their maximum available energy through MPPT algorithms. Finally, the new concepts of virtual impedance algorithms allow connecting several active powers in the same power grid running autonomously in decentralized microgrids, in a similar way as the generation systems sharing the load power.

Author details

Luís Fernando Corrêa Monteiro

Address all correspondence to: lmonteiro@uerj.br

Department of Electronics and Communications, Rio de Janeiro State University,
Rio de Janeiro, Brazil

References

- [1] Li H, Liu C, Li G, Annakkage U. Screening technique for identifying the risk of sub-synchronous resonance. *IET Generation, Transmission & Distribution*. 2016;**10**:1589-1596. DOI: 10.1049/iet-gtd.2015.0764
- [2] Sahraei-Ardakani M, Hedman KW. Computationally efficient adjustment of FACTS set points in DC optimal power flow with shift factor structure. *IEEE Transactions on Power Systems*. 2017;**32**:1733-1740. DOI: 10.1109/TPWRS.2016.2591503

- [3] Ghahremani E, Kamwa I. Analysing the effects of different types of FACTS devices on the steady-state performance of the Hydro-Québec network. *IET Generation, Transmission & Distribution*. 2014;**8**:233-249. DOI: 10.1049/iet-gtd.2013.0316
- [4] Gonzalez JM, Canizares CA, Ramirez JM. Stability modelling and comparative study of series vectorial compensators. *IEEE Transactions on Power Delivery*. 2010;**25**:1093-1103. DOI: 10.1109/TPWRD.2009.2034905
- [5] Wang L, Lam CS, Wong MC. Modelling and parameter design of thyristor-controlled LC-coupled hybrid active power filter (TCLC-HAPF) for unbalanced compensation. *IEEE Transactions on Industrial Electronics*. 2017;**64**:1827-1840. DOI: 10.1109/TIE.2016.2625239
- [6] Brandão DI, Guillard H, Morales-Paredes HK, Marafão FP, Pomilio JA. Optimized compensation of unwanted current terms by AC power converters under generic voltage conditions. *IEEE Transactions on Industrial Electronics*. 2016;**63**:7743-7753. DOI: 10.1109/TIE.2016.2594226
- [7] Marafão FP, Brandão DI, Costabeber A, Morales-Paredes HK. Multi-task control strategy for grid-tied inverters based on conservative power theory. *IET Renewable Power Generation*. 2015;**9**:154-165. DOI: 10.1049/iet-rpg.2014.0065
- [8] Khederzadeh M, Sadeghi M. Virtual active power filter: A notable feature for hybrid ac/dc microgrids. *IET Generation, Transmission & Distribution*. 2016;**10**:3539-3546. DOI: 10.1049/iet-gtd.2016.0217
- [9] Chilipi RR, Al Sayari N, Beig AR, Al Hosani K. A multitasking control algorithm for grid-connected inverters in distributed generation applications using adaptive noise cancellation filters. *IEEE Transactions on Energy Conversion*. 2016;**31**:714-727. DOI: 10.1109/TEC.2015.2510662
- [10] Zheng C, Zhou L, Yu X, Li B, Liu J. Online phase margin compensation strategy for a grid-tied inverter to improve its robustness to grid impedance variation. *IET Power Electronics*. 2016;**9**:611-620. DOI: 10.1049/iet-pel.2015.0196
- [11] Azzouz MA, El-Saadany EF. Multivariable grid admittance identification for impedance stabilization of active distribution networks. *IEEE Transactions on Smart Grid*. 2017;**8**:1116-1128. DOI: 10.1109/TSG.2015.2476758
- [12] Zhou L et al. Robust two degrees-of-freedom single-current control strategy for LCL-type grid-connected DG system under grid-frequency fluctuation and grid-impedance variation. *IET Power Electronics*. 2016;**9**:2682-2691. DOI: 10.1049/iet-pel.2016.0120
- [13] Chen X, Zhang Y, Wang S, Chen J, Gong C. Impedance-phased dynamic control method for grid-connected inverters in a weak grid. *IEEE Transactions on Power Electronics*. 2017;**32**:274-283. DOI: 10.1109/TPEL.2016.2533563
- [14] Tani A, Camara MB, Dakyo B. Energy management in the decentralized generation systems based on renewable energy—Ultracapacitors and battery to compensate the wind/load power fluctuations. *IEEE Transactions on Industry Applications*. 2015;**51**:1817-1827. DOI: 10.1109/TIA.2014.2354737

- [15] Chen L et al. Coordinated control of SFCL and SMES for transient performance improvement of microgrid with multiple DG units. *Canadian Journal of Electrical and Computer Engineering*. 2016;**39**:158-167. DOI: 10.1109/CJECE.2016.2520496
- [16] Silva-Saravia H, Pulgar-Painemal H, Mauricio JM. Flywheel energy storage model, control and location for improving stability: The Chilean case. *IEEE Transactions on Power Systems*. 2017;**32**:3111-3119. DOI: 10.1109/TPWRS.2016.2624290
- [17] Galeshi S, Iman-Eini H. Dynamic voltage restorer employing multilevel cascaded H-bridge inverter. *IET Power Electronics*. 2016;**9**:2196-2204. DOI: 10.1049/iet-pel.2015.0335
- [18] Komurcugil H, Biricik S. Time-varying and constant switching frequency-based sliding-mode control methods for transformerless DVR employing half-bridge VSI. *IEEE Transactions on Industrial Electronics*. 2017;**64**:2570-2579. DOI: 10.1109/TIE.2016.2636806
- [19] Oliveira SVG, Barbi I. A three-phase step-up DC-DC converter with a three-phase high-frequency transformer for DC renewable power source applications. *IEEE Transactions on Industrial Electronics*. 2011;**58**:3567-3580. DOI: 10.1109/TIE.2010.2084971
- [20] Tolbert LM, Peng FZ, Habetler TG. A multilevel converter-based universal power conditioner. *IEEE Transactions on Industrial Applications*. 2000;**36**:596-603. DOI: 10.1109/28.833778
- [21] Lee WC, Lee DM, Lee TK. New control scheme for a unified power-quality compensator-Q with minimum active power injection. *IEEE Transactions on Power Delivery*. 2010;**25**:1068-1076. DOI: 10.1109/TPWRD.2009.2031556
- [22] Ambati BB, Khadkikar V. Optimal sizing of UPQC considering VA loading and maximum utilization of power-electronic converters. *IEEE Transactions on Power Delivery*. 2014;**29**:1490-1498. DOI: 10.1109/TPWRD.2013.2295857
- [23] Akagi H, Nabae A, Atoh S. Control strategy of active power filters using multiple voltage-source PWM converters. *IEEE Transactions on Industry Applications*. 1986; **IA-22**:460-465. DOI: 10.1109/TIA.1986.4504743
- [24] Peng FZ, Akagi H, Nabae A. A study of active power filters using quad-series voltage-source PWM converters for harmonic compensation. *IEEE Transactions on Power Electronics*. 1990;**5**:9-15. DOI: 10.1109/63.45994
- [25] Tanaka T, Akagi H. A new method of harmonic power detection based on the instantaneous active power in three-phase circuits. *IEEE Transactions on Power Delivery*. 1995;**10**:1737-1742. DOI: 10.1109/61.473386
- [26] Cheng PT, Bhattacharya S, Divan D. Operations of the dominant harmonic active filter (DHAF) under realistic utility conditions. *IEEE Transactions on Industry Applications*. 2001;**37**:1037-1044. DOI: 10.1109/28.936394
- [27] Pigazo A, Moreno VM, Estebanez EJ. A recursive park transformation to improve the performance of synchronous reference frame controllers in shunt active power filters. *IEEE Transactions on Power Electronics*. 2009;**24**:2065-2075. DOI: 10.1109/TPEL.2009.2025335

- [28] Newman MJ, Zmood DN, Holmes DG. Stationary frame harmonic reference generation for active filter systems. *IEEE Transactions on Industry Applications*. 2002;**38**:1591-1599. DOI: 10.1109/TIA.2002.804739
- [29] Monteiro LFC, Aredes M, Pinto JG, Exposto BF, Afonso JL. Control algorithms based on the active and non-active currents for a UPQC without series transformers. *IET Power Electronics*. 2016;**9**:1985-1994. DOI: 10.1049/iet-pel.2015.0642
- [30] Moreno VM, Pigazo A. Modified FBD method in active power filters to minimize the line current harmonics. *IEEE Transactions on Power Delivery*. 2007;**22**:735-736. DOI: 10.1109/TPWRD.2006.886769
- [31] Monteiro LFC, Afonso JL, Pinto JG, Watanabe EH, Aredes M, Akagi H. Compensation algorithms based on the p-q and CPC theories for switching compensators in micro-grids. In: *Proceedings of the Brazilian Power Electronics Conference (COBEP'09)*, 2009. Mato Grosso, Brazil, pp. 32-40. DOI: 10.1109/COBEP.2009.5347593
- [32] Herrera RS, Salmeron P. Instantaneous reactive power theory: A comparative evaluation of different formulations. *IEEE Transactions on Power Delivery*. 2007;**22**:595-604. DOI: 10.1109/TPWRD.2006.881468
- [33] Herrera RS, Salmeron P, Kim H. Instantaneous reactive power theory applied to active power filter compensation: Different approaches, assessment, and experimental results. *IEEE Transactions on Industrial Electronics*. 2008;**55**:184-196. DOI: 10.1109/TIE.2007.905959
- [34] Xu Y, Tolbert LM, Chiasson JN, Campbell JB, Peng FZ. A generalised instantaneous non-active power theory for STATCOM. *IET Electric Power Applications*. 2007;**1**:853-861. DOI: 10.1049/iet-epa:20060290
- [35] Konstantopoulos GC, Zhong QC, Ming WL. PLL-less nonlinear current-limiting controller for single-phase grid-tied inverters: Design, stability analysis, and operation under grid faults. *IEEE Transactions on Industrial Electronics*. 2016;**63**:5582-5591. DOI: 10.1109/TIE.2016.2564340
- [36] Hadjidemetriou L, Kyriakides E, Blaabjerg F. An adaptive tuning mechanism for phase-locked loop algorithms for faster time performance of interconnected renewable energy sources. *IEEE Transactions on Industry Applications*. 2015;**51**:1792-1804. DOI: 10.1109/TIA.2014.2345880
- [37] Carneiro H, Monteiro LFC, Afonso JL. Comparisons between synchronizing circuits to control algorithms for single-phase active converters. In: *Proceedings of the IEEE Conference on Industrial Electronics (IECON'09)*; 3229-3234, 2009. Porto, Portugal. DOI: 10.1109/IECON.2009.5415214
- [38] Karimi-Ghartemani M et al. A new phase-locked loop system for three-phase applications. *IEEE Transactions on Power Electronics*. 2013;**28**:1208-1218. DOI: 10.1109/TPEL.2012.2207967
- [39] Freitas CM, Monteiro LFC, Watanabe EH. A novel current harmonic compensation based on resonant controllers for a selective active filter. In: *Proceedings of the IEEE Conference*

on Industrial Electronics (IECON'16), 2016, Florence, Italy, pp. 3666-3671. DOI: 10.1109/IECON.2016.7793519

- [40] Perera B, Ciufo P, Perera S. Advanced point of common coupling voltage controllers for grid-connected solar photovoltaic (PV) systems. *Renewable Energy*. 2016;**86**:1037-1044. DOI: 10.1016/j.renene.2015.09.028
- [41] Abdullah MA et al. A review of maximum power point tracking algorithms for wind energy systems. *Renewable and Sustainable Energy Reviews*. 2012;**16**:3220-3227. DOI: 10.1016/j.rser.2012.02.016
- [42] Zhang Y, Yu M, Liu F, Kang Y. Instantaneous current-sharing control strategy for parallel operation of UPS modules using virtual impedance. *IEEE Transactions on Power Electronics*. 2013;**28**:432-440. DOI: 10.1109/TPEL.2012.2200108

IntechOpen